International Journal of Control and Automation
Vol.10, No.6 (2017), pp.219-230
http://dx.doi.org/10.14257/ijca.2017.10.6.21

X-ray Pulsar Based Navigation using Online Optimization

Jin Jing, Xiaoyu Li and Yi Shen

Department of Control Science and Engineering,
Harbin Institute of Technology, Harbin
jinjinghit@hit.edu.cn

Abstract

To improve the performance X-ray pulsar based navigation system (XNAV) with the shuttered problem, an UKF filtering algorithm with multiple model optimal estimation (MMOE) method is proposed. Through analyzing the impact of measurement with shuttered pulsar to UKF, the scheme with multiple measurement models is propose and the UKF-MMOE based method is designed to deal with the measurement in presents of shuttered pulsar. The proposed method is tested on the Mars rotation orbit and compared with the conventional UKF based filtering algorithm. Simulation results demonstrated that the proposed method decrease the influence of measurement with shuttered pulsar to navigation system and achieve higher estimation performance than using UKF.

Keywords: *X-ray pulsar; autonomous navigation; pulsar direction error; UKF; online pulsar optimization*

1. Introduction

X-ray pulsar-based navigation (XNAV) is a newly emerging autonomous navigation technology, using X-ray pulsar as its navigation source [1]. Compared with existing autonomous navigation technologies, such as inertial navigation and celestial navigation [2-3], XNAV has the advantages of high reliability, high precision and strong autonomy [4]. Thus, XNAV has become a hot research subject in the autonomous navigation field.

X-ray pulsars are rapidly rotating neutron stars emitting the signal in X band, which can be detected by X-ray sensors fixed onboard spacecraft [5]. The pulsed signals can be processed by the spacecraft to obtain the pulsar's time-of-arrival (TOA) after a period of observation (usually lasts about 5-10 min) [6]. The pulsar's corresponding time at the solar system barycenter (SSB) can be predicted in a high accuracy by the pulse phase timing model. Therefore, the offset of a pulse TOA at the spacecraft compared to its corresponding time at the SSB can be calculated [7]. It is the time offset that is used as the basic measurement in XNAV [8]. Using a specific navigation filtering algorithm, the spacecraft's position and velocity can be accurately estimated.

Without considering the system bias, Sheikh has applied KF as navigation filter to XNAV to estimate the orbit parameters in real time and has achieved the positioning accuracy of 200m [9]. Qiao Li has introduced the EKF to XNAV by expanding the Taylor series in the nonlinear dynamic model [10]. However, the linearization error can severely decrease the performance of EKF since the high order term of Taylor series are neglected. To solve the problem, the UKF-based method which is implemented to obtain the mean and covariance estimations with a set of sigma points [11] is more suitable for the nonlinear dynamic model in practice application and can effectively reduce the impact of linearization errors.

However, for the Mars rotation orbit, the X-ray pulsar may be blocked by the Mars and the pulsar signal cannot be received by the sensor. In previous studies, the pulsar shutter problem has rarely been taken into account, especially in the Mars rotation orbit. The traditional Geometric Dilution of Precision (GDOP) [12] based method can solve the

ISSN: 1738-9984 IJCA

problem in Mars rotation orbit based on the ideal that the adopted pulsars are pre-selected before the spacecraft is launched. The GDOP is an offline method and not suitable for the complex Mars exploration.

In order to solve this problem, a novel unscented Kalman filtering algorithm with multiple measurement model optimization method is proposed. By selecting appropriate pulsars with the online method, the optimal combination of pulsars can be adaptively chosen and further the navigation performance of ordinary UKF is greatly improved in presents of the X-ray pulsar is shuttered by the Mars.

This paper is organized as follows. In Section 2, the dynamical model and measurement model of XNAV are given and the navigation error analysis is introduced. In Section 3, the proposed navigation method based on UKF and online pulsar optimization is designed. The effectiveness of the proposed method is demonstrated through simulations in Section 4. Finally, the conclusions are drawn in Section 5.

2. Formatting your Paper

The purpose of XNAV is to estimate the orbit states of spacecrafts in real time, such as the position and velocity. The orbit dynamic model and measurement model used in the navigation procedure are introduced in detail.

2.1. Orbit Dynamic Model

The state vector $\boldsymbol{X}=[\boldsymbol{r}\ \ \boldsymbol{v}]^T$ is composed by position vector $\boldsymbol{r}=[x\ \ y\ \ z]^T$ and velocity vector $\boldsymbol{v}=[v_x\ \ v_y\ \ v_z]^T$ in the Mars-centered inertial coordinate system (J2000.0). The common state equation of the spacecraft navigation system is given as

$$\begin{cases} \dot{x}=v_x \\ \dot{y}=v_y \\ \dot{z}=v_z \\ \dot{v}_x=-\dfrac{\mu_m x}{\|\boldsymbol{r}\|^3}\left[1+J_2\left(\dfrac{R_m}{\|\boldsymbol{r}\|}\right)^2\dfrac{3}{2}\left(1-5\dfrac{z^2}{\|\boldsymbol{r}\|^2}\right)\right]+\Delta F_x \\ \dot{v}_y=-\dfrac{\mu_m y}{\|\boldsymbol{r}\|^3}\left[1+J_2\left(\dfrac{R_m}{\|\boldsymbol{r}\|}\right)^2\dfrac{3}{2}\left(1-5\dfrac{z^2}{\|\boldsymbol{r}\|^2}\right)\right]+\Delta F_y \\ \dot{v}_z=-\dfrac{\mu_m z}{\|\boldsymbol{r}\|^3}\left[1+J_2\left(\dfrac{R_m}{\|\boldsymbol{r}\|}\right)^2\dfrac{3}{2}\left(3-5\dfrac{z^2}{\|\boldsymbol{r}\|^2}\right)\right]+\Delta F_z \end{cases} \tag{1}$$

where $\Delta\boldsymbol{F}=[\Delta F_x\ \ \Delta F_y\ \ \Delta F_z]^T$ is the high-order perturbation acceleration of spacecraft, including non-spherical perturbation of Earth, sun pressure, the third-body gravitational perturbation *etc.*, R_m is the radius of the Earth, μ_m is the gravitational coefficient of Earth and J_2 is the second order zonal coefficient.

2.2. Measurement Model

The XNAV principle based on the pulsar optimization is described in Figure 1. The measurement model is obtained by processing the offset of TOA between the spacecraft and SSB. $\boldsymbol{n}_j$ is the directional vector of the j th pulsar, $\boldsymbol{R}_{SC}$ is the position vector of spacecraft relative to the SSB. The pulses emitted by the j th

pulsar spread from the spacecraft to the SSB, where the delay of TOA denotes the projection of $\boldsymbol{R}_{SC}$ along the direction vector of pulsars. The time transfer equation can be described as

$$y_j = c\left(t_{SSB}^j - t_{SC}^j\right) = \boldsymbol{n}_j \boldsymbol{R}_{SC} \tag{2}$$

where c is the speed of light, $\boldsymbol{n}_j = [\cos\delta^j \sin\alpha^j \quad \cos\delta^j \cos\alpha^j \quad \sin\delta^j]$ is the pulsar direction vector, α is the right ascension, δ is the declination. $\boldsymbol{R}_{SC}$ can be obtained by

$$\boldsymbol{R}_{SC} = \boldsymbol{r} + \boldsymbol{r}_m \tag{3}$$

where $\boldsymbol{r}_m$ is the distance from SSB to Mars and can be obtained by the JPL DE 405 ephemeris, $\boldsymbol{r}$ is the distance from spacecraft to the Mars.

In this paper, $c(t_{SSB}^j - t_{SC}^j)$ is selected as measurement vector, then the measurement equation based on the observations of four pulsars can be expressed as

$$\boldsymbol{y}(t) = \boldsymbol{h}\left(\boldsymbol{X}(t)\right) + \boldsymbol{\eta}(t) \tag{4}$$

where $\boldsymbol{y}(t) = \left[y_1 \quad y_2 \quad \cdots \quad y_m\right]^T$, $h_j\left(\boldsymbol{X}(t)\right) = \boldsymbol{n}_j \boldsymbol{R}_{SC}$, $j = 1, \cdots, m$, m is the number of configured pulsar detectors in spacecraft. $\boldsymbol{\eta}(t)$ is the measurement noise which obeys the zero mean Gaussian distribution.

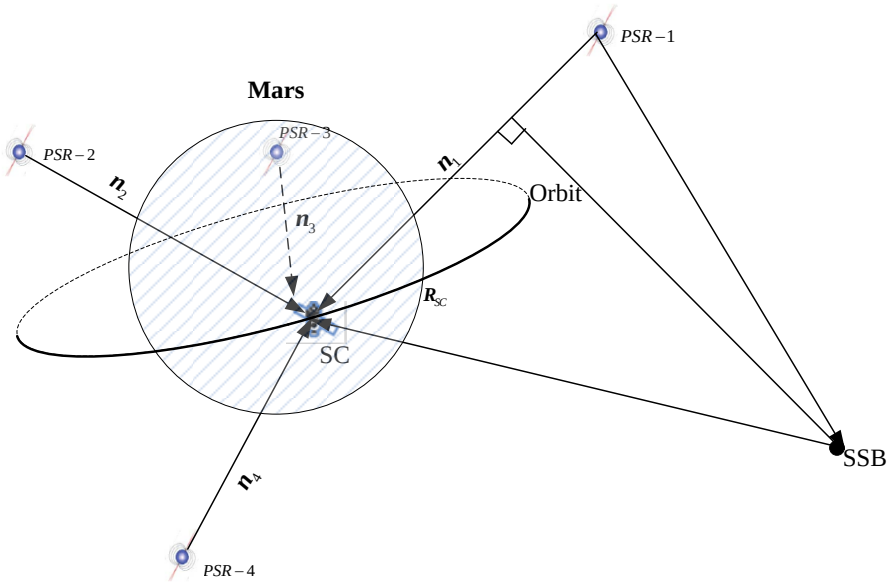

Figure 1. Illustration of the XNAV based on Pulsar Selection

2.3. Analysis on Shuttered Problem

As illustrated in Figure 1, at least three pulsar measurements are adopted for once navigation filtering procedure. If one of the adopted three pulsars is shuttered by the Mars, the performance of UKF will be severely affected. Thus, an optimal combination is needed to be optimized from the candidate pulsars.

Figure 2 (a) illustrates the problem. As the pulsars are very far from the orbit, the pulsar's signal is supposed to transmit in parallel. When the pulsar emits X-ray signal, there is a cylinder area on the back of the Earth where the spacecraft cannot receive the signal accurately. In Figure 4 (a) the green, red and yellow areas

correspond to the shuttered regions of the pulsar 1, 2 and 3 respectively. If the spacecraft flies into one of the cylinder area, the corresponding measurement signal will be faulty and will lead to navigation failure.

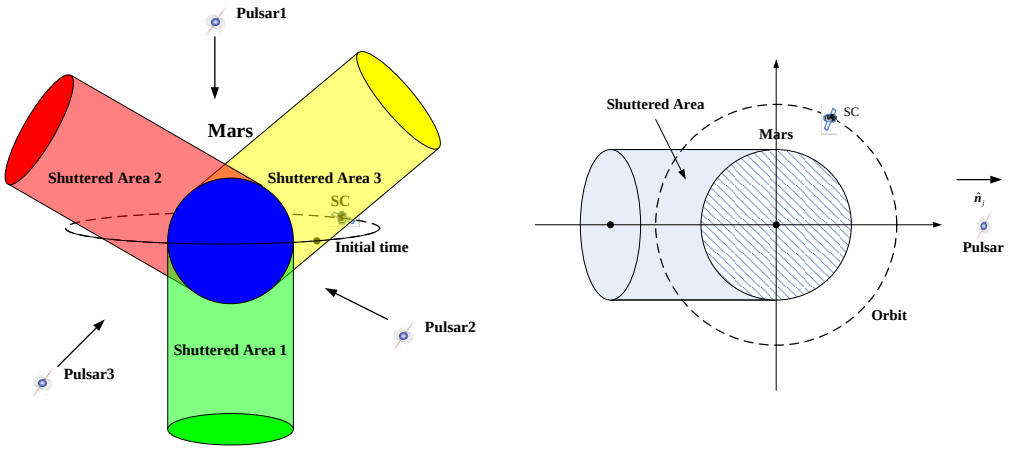

(a) (b)

Figure 2. The Illustration on Shutter Issue

In order to determine the location of the shuttered area precisely, the J2000.0 coordinate system is transmitted, X axis' directs the j th pulsar $\hat{\boldsymbol{n}}_j$ as shows in Figure 2. (b). Suppose the position of spacecraft in J2000.0 is $\boldsymbol{r}_k = [x_k \quad y_k \quad z_k]^T$, then the position of spacecraft in Fig.2 (b) system is changed into:

$$\begin{cases} R_{x,k}^{(j)} = x_k \cos(\hat{\delta}^{(j)})\cos(\hat{\alpha}^{(j)}) \\ R_{y,k}^{(j)} = y_k \cos(\hat{\delta}^{(j)})\sin(\hat{\alpha}^{(j)}) \\ R_{z,k}^{(j)} = z_k \sin(\hat{\delta}^{(j)}) \end{cases} \tag{5}$$

where $\hat{\alpha}^{(j)}$ and $\hat{\delta}^{(j)}$ are the right ascension and declination of the j th pulsar. If the spacecraft enters into the shuttered area of the j th pulsar, the spacecraft's position in the rotated coordinate system need to meet the following two conditions:

$$\begin{cases} (R_{y,k}^{(j)})^2 + (R_{z,k}^{(j)})^2 \le R_m^2 \\ R_{x,k}^{(j)} \le 0 \end{cases} \tag{6}$$

where R_m is the radius of the Mars.

When the spacecraft is trapped into the shuttered area, the sensor located in the spacecraft cannot receive the valid photon emitted from the corresponding pulsar but only the background noise. Therefore, it is unable to form an effective accumulated profile to estimate the time offset. According to the equation (2) and (3), for the Mars rotation orbit, $|\boldsymbol{r}_m| \square |\boldsymbol{r}|$, so the measurement's amplitude can be illustrated as:

$$|y_j| = \left|c\left(t_{SSB}^j - t_{SC}^j\right)\right| = \left|\boldsymbol{n}_j\left(\boldsymbol{r}_m + \boldsymbol{r}\right)\right| \approx \left|\boldsymbol{n}_j \cdot \boldsymbol{r}_m\right| \tag{7}$$

Thus, the paper assumes to use a Gaussian distribution as the substitute for the measurement with the probability density function given by:

$$f(y_j) = \frac{1}{\sqrt{2\pi}\left|\boldsymbol{n}_j \cdot \boldsymbol{r}_E\right|} \exp\left(\frac{-y_j}{2\left|\boldsymbol{n}_j \cdot \boldsymbol{r}_E\right|^2}\right) \tag{8}$$

For the Mars rotation orbit, Figure 3 shows the pulsar's visibility and the corresponding condition of measurement. The number "0" represents an X-ray pulsar is shuttered by the Mars which is shown in Figure 3 (a) and the number "1" represents the other case as described in Figure 3 (b). When the pulsar signal is shuttered by the Mars, the photon cannot be obtained by the X-ray detector and the corresponding measurement will be generated randomly by the equation (8).

The navigation results of UKF for the two cases are shown in Figure 6. Figure 6 (a) shows the X-ray pulsar is not shuttered by the Mars. The navigation system works well and the estimation error is a few hundred meters without considering the occlusion. For the other case, when the shuttered problem is taken into account, the estimation error severely increases to 8×10^6 meters, which is shown in Figure 6 (b) This means the shutter issue will generate very poor navigation performance even lead to system instability.

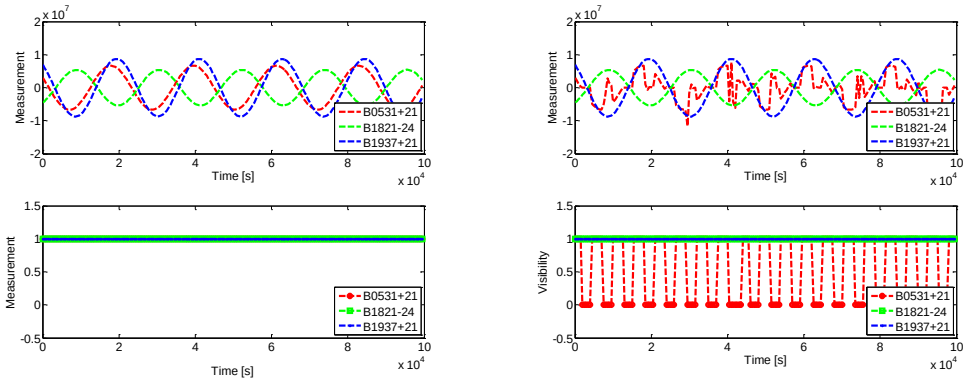

(a) (b)

Figure 3. The Difference between Pulsar's Measurements without Shutter (a) and with Shutter (b)

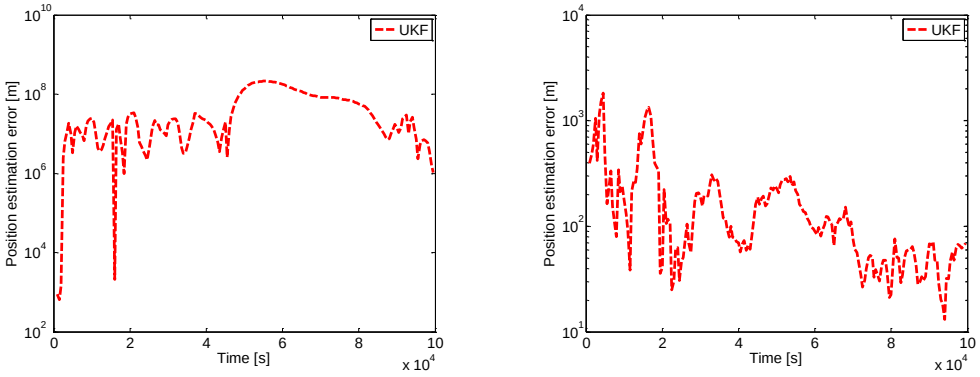

(a) (b)

Figure 4. The Estimation Errors of UKF without Shutter (a) and with Shutter (b)

Based on the above analysis, the shuttered pulsar signal is the main factors influencing the navigation accuracy of XNAV. Therefore, it is of great significance

to design a corresponding filter to eliminate the impacts of shuttered problem mentioned above.

3. Navigation Method based on UKF Parallel Filtering and Online Pulsar Optimization

In order to overcome the problems, a navigation method based on parallel UKF filtering algorithm and online pulsar optimization method is proposed. The main procedure of the proposed method is shown in Figure 7. Firstly, four pulsars are selected from the existing pulsar model database and recorded as pulsar1~pulsar4. Then four pulsar combinations, recorded as A1~A4, are formed using the method listed in the Table 1. After that, four filters can be obtained based on the UKF method, and the corresponding navigation parameters in the current measurement update are acquired. Finally, the proposed online pulsar optimization method is used to obtain the optimal navigation result of the four UKFs.

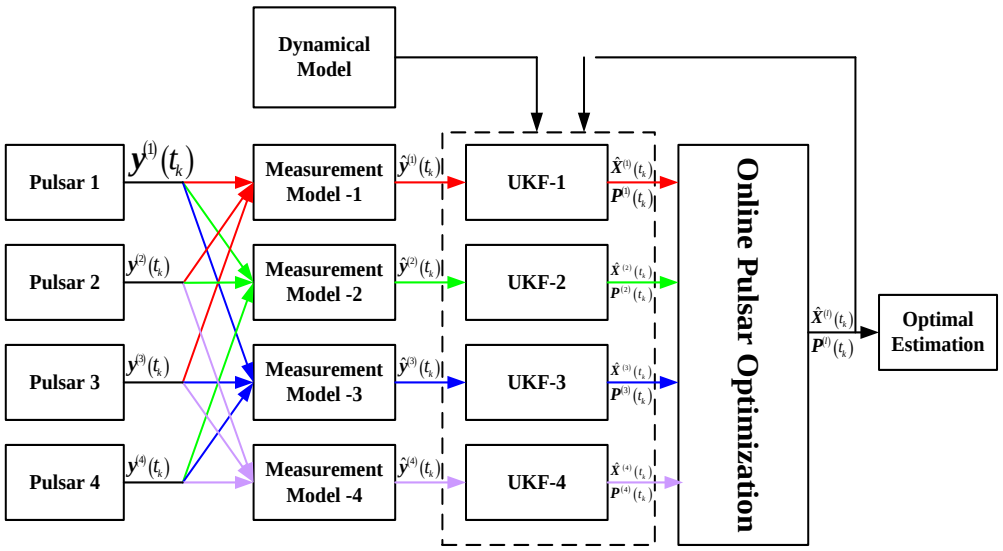

Figure 5. Procedure of the Proposed Method

Table 1. List of Pulsar Combinations

Pulsar Combinations	Combination method			
	A^1	A^2	A^3	A^4
B0531+21	√	√	√	×
B1821-24	√	√	×	√
B1937+21	√	×	√	√
B1636-536	×	√	√	√

3.1. Parallel Filtering

According to Section 2.1 and 2.2, the XNAV can be written in general as:

$$\begin{cases} \boldsymbol{x}_k = f(\boldsymbol{x}_{k-1}) + \boldsymbol{w}_k \\ \boldsymbol{y}_k = \boldsymbol{H}_k \boldsymbol{x}_k + \boldsymbol{V}_k \end{cases} \tag{9}$$

where $\boldsymbol{x}_k \in \mathbf{R}^n$ and $\boldsymbol{y}_k \in \mathbf{R}^n$ are the system state and the measurement, respectively. $f(\square)$ is the nonlinear dynamical model in general. $\boldsymbol{w}_k$ and $\boldsymbol{V}_k$ are the process and

measurement noise with the covariance $\boldsymbol{Q}_k$ and $\boldsymbol{R}_k$ respectively. Then, the UKF parallel filtering algorithm is described as follows:

Initialization: For the state vector $\boldsymbol{x}_{k-1}$ of XNAV with the mean $\hat{\boldsymbol{x}}_{k-1}$ and covariance $\hat{\boldsymbol{P}}_{k-1}$, the sigma point is processed with the unscented transform (UT):

$$\begin{cases} \boldsymbol{\chi}_{i,k-1} = \hat{\boldsymbol{x}}_{k-1} & i = 0 \\ \boldsymbol{\chi}_{i,k-1} = \hat{\boldsymbol{x}}_{k-1} + (a\sqrt{n\hat{\boldsymbol{P}}_{k-1}})_i & i = 1,...,n \\ \boldsymbol{\chi}_{i,k-1} = \hat{\boldsymbol{x}}_{k-1} - (a\sqrt{n\hat{\boldsymbol{P}}_{k-1}})_{i-n} & i = n+1,...,2n \end{cases} \tag{10}$$

where $(a\sqrt{n\hat{\boldsymbol{P}}_{k-1}})_i$ is the i th column of the matrix $\sqrt{n\hat{\boldsymbol{P}}_{k-1}}$, a is the tuning parameter, in this paper, a is set to 0.1.

Prediction: For each sigma point, it is processed with the dynamical model in (1)

$$\boldsymbol{\chi}_{i,k/k-1} = f(\boldsymbol{\chi}_{i,k-1}) \tag{11}$$

Thus, the prediction mean and covariance is written as:

$$\hat{\boldsymbol{x}}_{k/k-1} = \sum_{i=0}^{2n} \omega_i \boldsymbol{\chi}_{i,k/k-1} \tag{12}$$

$$\hat{\boldsymbol{P}}_{k/k-1} = \sum_{i=0}^{2n} \omega_i (\boldsymbol{\chi}_{i,k/k-1} - \hat{\boldsymbol{x}}_{k/k-1})(\boldsymbol{\chi}_{i,k/k-1} - \hat{\boldsymbol{x}}_{k/k-1})^T + \boldsymbol{Q}_k \tag{13}$$

where $\begin{cases} \omega_i = 1-(1/a^2) & i = 0 \\ \omega_i = 1/2na^2 & i = 1,...,2n \end{cases}$.

Measurement update: As the measurement model of XNAV is linear, each UKF updates the state and covariance in parallel individually, the measurement update step is summarized as follows:

$$\hat{\boldsymbol{y}}_{k/k-1}^{(i)} = \boldsymbol{H}_k^{(i)} \hat{\boldsymbol{x}}_{k/k-1} \tag{14}$$

$$\boldsymbol{P}_{yy}^{(i)} = \boldsymbol{H}_k^{(i)} \boldsymbol{P}_{k/k-1} (\boldsymbol{H}_k^{(i)})^T + \boldsymbol{R}_k^{(i)} \tag{15}$$

$$\boldsymbol{P}_{xy}^{(i)} = \boldsymbol{P}_{k/k-1} (\boldsymbol{H}_k^{(i)})^T \tag{16}$$

$$\boldsymbol{K}_k^{(i)} = \boldsymbol{P}_{xy}^{(i)} (\boldsymbol{P}_{yy}^{(i)})^{-1} \tag{17}$$

$$\hat{\boldsymbol{x}}_k^{(i)} = \hat{\boldsymbol{x}}_{k/k-1} + \boldsymbol{K}_k^{(i)} (\boldsymbol{y}_k^{(i)} - \hat{\boldsymbol{y}}_{k/k-1}^{(i)}) \tag{18}$$

$$\boldsymbol{P}_k^{(i)} = \boldsymbol{P}_{k/k-1} - \boldsymbol{K}_k^{(i)} \boldsymbol{P}_{yy}^{(i)} (\boldsymbol{K}_k^{(i)})^T \tag{19}$$

where i is the number of adopted measurement combinations.

3.2. Online Pulsar Optimal Estimation

Traditional pulsar selection method is based on the offline manner. Firstly, several pulsars are selected based on the optimizing criteria of pulsar selection, forming the navigation pulsar database. Secondly, the GDOP for different pulsar combinations is calculated. Finally, the optimal pulsar combination can be obtained through selecting the minimum value of the GDOP. This means the navigation pulsars are unchanged in the whole process of filtering.

However, since the position of spacecraft varies with time, the used pulsars should also be adjusted dynamically in order to match the orbit and avoid the shuttered areas. The proposed parallel filter bank of UKFs can provide multiple

measurement estimations $\boldsymbol{y}_k^{(i)}$ based on the measurement model. There will be a large disparity in each measurement residual $\tilde{\boldsymbol{y}}_k^{(i)}$ ($\tilde{\boldsymbol{y}}_k^{(i)} = \boldsymbol{y}_k^{(i)} - \hat{\boldsymbol{y}}_k^{(i)}$). Thus, the optimal estimation index function is established based on the measurement residuals and is defined as:

$$e_k^{(i)} = \frac{1}{\sqrt{2\pi(\tilde{\boldsymbol{y}}_k^{(i)})^T \boldsymbol{\Omega}_k^{(i)} \tilde{\boldsymbol{y}}_k^{(i)}}} \exp\left[-\frac{1}{2} (\tilde{\boldsymbol{y}}_k^{(i)})^T \boldsymbol{\Omega}_k^{(i)} \tilde{\boldsymbol{y}}_k^{(i)} \right] \tag{20}$$

where $\tilde{\boldsymbol{y}}_k^{(i)} = \boldsymbol{y}_k^{(i)} - \hat{\boldsymbol{y}}_k^{(i)}$ represents the i th filter's measurement residual, $\boldsymbol{\Omega}_k^{(i)}$ is the corresponding covariance. According to the Eq. (14), the residual control variable of UKFs' filters can be calculated and recorded as:

$$\boldsymbol{e}_k = [e_k^{(1)} \quad e_k^{(2)} \quad e_k^{(3)} \quad e_k^{(4)}] \tag{21}$$

Afterwards, the index function is established based on the maximum estimation error criterion, which is shown as

$$[\sim, l] = max\{\boldsymbol{e}_k\} \tag{22}$$

where $l \in \{1,2,3,4\}$ denotes the identifier of the optimal pulsar combination.

Assume that the final estimated state and covariance is recorded as $\hat{\boldsymbol{x}}_k$ and $\boldsymbol{P}_k$ respectively, then the final optimal state for a specific spacecraft is determined based on the following equation:

$$\begin{cases} \hat{\boldsymbol{x}}_k = \hat{\boldsymbol{x}}_k^{(l)} \\ \boldsymbol{P}_k = \boldsymbol{P}_k^{(l)} \end{cases} \tag{23}$$

In the iteration the optimization strategy is used to correct and filter the preferred state. The residual control index $e_k^{(i)}$ can sense the difference between the measured and the predicted measurements. Through maximizing the residual control index, the estimated system state will be close to the actual and optimal ones. Especially, when a pulsar is shuttered, the strategy can still ignore the impact of the fault signal and can obtain an optimal state estimation from another measurement.

4 Simulation and Results Analysis

4.1. Simulation Conditions

In order to demonstrate the effectiveness of the proposed method, three existing high Earth orbits OPS-5111, GGTS and INTELSAT2-F2 [13] are selected and compared with the UKF method. The simulation time and basic elements of the selected orbits are generated by the STK and listed in Table 2 and Table 3. The parameters of the selected pulsars are shown in Table 4 (Observing conditions: the X-ray sensor's area is $1m^2$, X-ray background is 0.005 $ph/cm^2/s$).

The simulation parameters are given as follows:

(1) Measurement update: 500s;

(2) Initial state errors: $\delta\hat{\boldsymbol{x}}_0 = [1000,1000,1000,2,2,2]^T$

(3) The initial error covariance $\boldsymbol{P}_0$, system noise covariance $\boldsymbol{Q}_k$ and measurement noise covariance $\boldsymbol{R}_k$ are:

$$\begin{cases} \boldsymbol{P}_0 = diag(1000^2, 1000^2, 1000^2, 2^2, 2^2, 2^2) \\ \boldsymbol{Q}_k = diag(10^{-2}, 10^{-2}, 10^{-2}, 10^{-4}, 10^{-4}, 10^{-4}) \\ \boldsymbol{R}_k = diag(109^2, 325^2, 298^2, 302^2) \end{cases} \tag{24}$$

Table 2. Elements of Mars Rotation Orbit

	Orbit 1	Orbit 2
Semi-major axis [km]	15000	6794
Eccentricity	0.05	0.1
Inclination [°]	30	45
Right ascension of ascending node [°]	30	0
The argument of perigee [°]	30	0
True anomaly [°]	0	30

Table 3. Parameters of Adopted Pulsars

Pulsars	Right ascension [°]	Declination [°]	Ranging accuracy [m]
B0531+21	88.63	22.01	109
B1821-24	276.13	-24.87	325
B1937+21	294.92	21.58	298
B1636-536	250.23	-53.74	302

Root mean square error is used to evaluate the navigation performance. Define the estimation error square root of position and velocity as

$$\begin{cases} \mathrm{RMSE}_r = \sqrt{\sum_{j=1}^{M} \left\| \Delta \boldsymbol{r}_j \right\|^2} \\ \mathrm{RMSE}_v = \sqrt{\sum_{j=1}^{M} \left\| \Delta \boldsymbol{v}_j \right\|^2} \end{cases} \tag{25}$$

where $\Delta \boldsymbol{r}$ and $\Delta \boldsymbol{v}$ are the estimation error of position and velocity. M is the length of the selected filtering interval.

4.2. Results Analysis

In order to verify the performance of the proposed method, the four UKFs and UKF-MMOE based method are compared and tested on the two Mars rotation orbits. The navigation results in orbit 1 are shown in Figure 9. The four UKFs all cannot converge in case of the navigation pulsar is shuttered, the navigation performance is severely affected. Meanwhile, for the proposed UKF-MMOE based method, the position and velocity estimation error all can converge and the navigation performance is improved.

In order to further verify the effectiveness of UKF-MMOE, another Mars rotation orbit (Orbit 2) is introduced. Figure 4 shows the performance of comparison for four UKF and UKF-MMOE. Same as the result in Orbit 1, the UKF-1 to UKF-4 still suffer from low accuracy navigation result. It is clear that the UKF-based method greatly degrades the navigation performance, while the UKF-MMOE filtering algorithm can still reach the steady state. These suggest that the proposed method can effectively deal with the impact of shuttered pulsars to XNAV.

In order to further verify the performance of this method, the RMSE_r and RMSE_v are calculated in Table 4. The position and velocity estimation error of UKF is sharply to 2.5083×10^8 and 1.0768×10^4, the corresponding estimation error of UKF-MMOE is 323.0075 and 0.1858. The reason is that the measurement in UKF is severely interfered in case that the pulsar is shuttered by Mars, which leads to the mutation of measurement

residual and further the failure of estimation. For the UKF-MMOE based method, the multiple measurement models is adopted, the Optimization method can always select the measurement which is not shuttered by the celestial body based on the residuals.

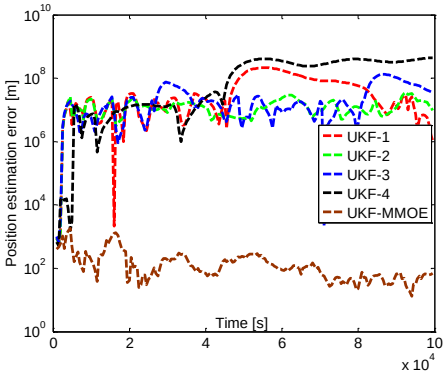

(a) Position Estimation Error

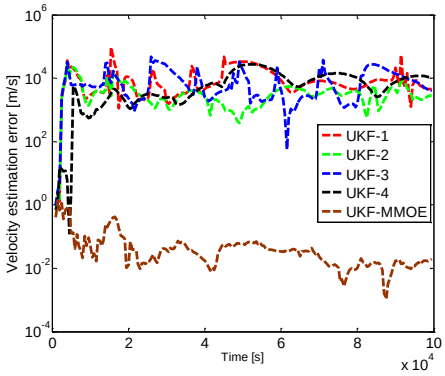

(b) Velocity Estimation Error

Figure 6. Estimation Result in Orbit 1

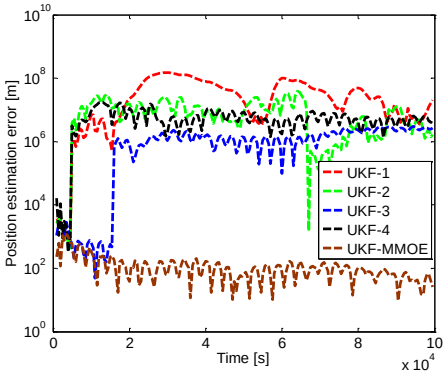

(a) Position Estimation Error

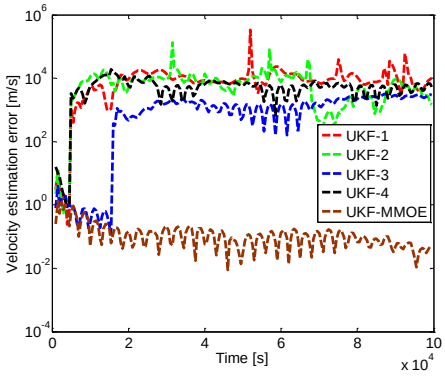

(b) Velocity Estimation Error

Figure 7. Estimation Result in Orbit 2

Table 4. RMSE of the Two Filtering Methods

Orbit	Orbit 1		Orbit 2	
	$RMSE_r$ (m)	$RMSE_v$ (m/s)	$RMSE_r$ (m)	$RMSE_v$ (m/s)
UKF-1	8.0069×10^7	1.5682×10^4	6.0548×10^7	2.6791×10^4
UKF-2	1.4619×10^7	5.4265×10^3	1.2925×10^7	1.4241×10^4
UKF-3	4.2614×10^7	1.3005×10^4	1.5660×10^6	1.6519×10^3
UKF-4	2.5083×10^8	1.0768×10^4	6.8792×10^6	6.3925×10^3
UKF-MMOE	323.0075	0.1858	211.0563	0.2301

In order to compare the computation time of the proposed strategy with the original UKF, the same hardware and software platform was used to test the filtering codes, where the CPU is Pentium E5300 2.6GHz, the RAM is 2GB, the MATLAB version is 2010a. Figure 6 shows the average time of running ten times of every filtering method. In the figure every independent UKF takes almost the same time (about 8.5 seconds), while the proposed method consumes more time than the single one (about 9.5 seconds). Although the proposed method has four parallel UKF filters, but their dynamical models are the same, and therefore, only one prediction procedure is used to complete state estimation. In

addition, the time of measurement update in XNAV is usually 300-500s, so the proposed method can fully meet the requirement in real navigation procedure.

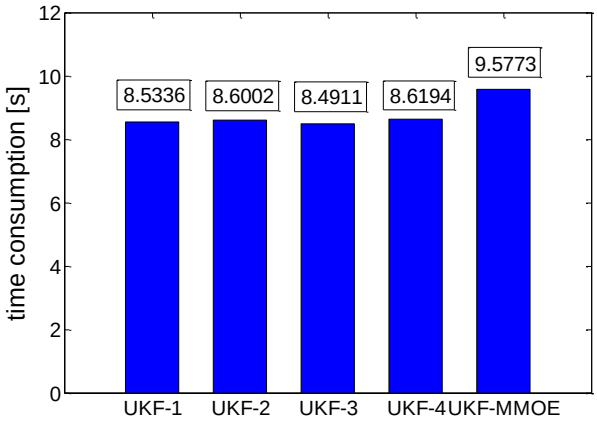

Figure 8. Time Consumption of the Filtering Algorithm

5. Conclusions

In this paper, an X-ray pulsar-based navigation method is proposed based on the UKF and online pulsar selection. The online pulsar selection method is designed to dynamically select the pulsar combinations based on the established index function. The simulation results show that the proposed method can effectively compensate the impact of the shuttered problem by the celestial body and get higher accuracy than UKF.

Acknowledgments

This work was supported by the innovation fund of China Aerospace Science and Technology Corporation - Harbin Institute of Technology Joint Innovation Center [CASC-HIT-1C04].

References

[1] P. Shuai, S. Chen, Y. Wu, C. Zhang and M. Li, "Navigation principles using X-ray pulsars", Journal of Astronaut, vol. 6, **(2007)**, pp. 1538-1543.
[2] Z. Wang, W. Wang, C. Hu, X. Si and J. Li, "A real-time prognostic method for the drift errors in the inertial navigation system by a nonlinear random-coefficient regression model", Acta Astronautica, vol. 103, **(2014)**, pp. 45-54.
[3] X. Ning and J. Fang, "A new automous celestial navigation method for the lunar rover", Robotics and Autonomous Systems, vol. 57, no. 1, **(2009)**, pp. 48-54.
[4] D. N. Matsakis, J. H. Taylor and T. M. Eubanks, "A statistic for describing pulsar and clock stabilities, Astronomy and Astrophysics", vol. 326, **(1997)**, pp. 924-928.
[5] S. I. Sheikh and D. J. Pines, "Recursive estimation of spacecraft position and velocity using x-ray pulsar time of arrival measurements", Navigation, vol. 53, no. 3, **(2006)**, pp. 149-166.
[6] L. Liu, W. Zheng and G. Tang, "Observability analysis of satellite constellations autonomous navigation based on X-ray pulsar measurement", Chinese Automation Congress, Changsha, China, **(2013)**, November 7-8.
[7] A. A. Emadzadeh and J. L. Speyer, "On modeling and pulse phase estimation of X-ray pulsars", IEEE Transactions on Signal Processing, vol. 58, no. 9, **(2010)**, pp. 4484-4495.
[8] A. A. Emadzadeh and J. L. Speyer, "Consistent estimation of pulse delay for X-ray pulsar based relative navigation", IEEE Decision and Control& Chinese Control Conference, **(2009)** December 16-18.
[9] S. I. Sheikh, D. J. Pines, P. S. Ray, K. S. Wood, M. N. Lovellette and M. T. Wolff, "Spacecraft naviagiton using x-ray pulsars", Journal of Guidance Control and Dynamics, vol. 29, no. 1, **(2006)**, pp. 49-63.

[10] L. Qiao, J. Liu, G. Zheng and Z. Xiong, "Augmentation of XNAV system to an ultraviolet sensor-based satellite navigation system", IEEE Journal of Selected Topics in Signal Processing, vol. 5, no. 3, **(2009)**, pp. 777-785.
[11] J. Liu, J. Ma, J. Tian, Z. Kang and P. White, "Pulsar navigation for interplanetary missions using CV model and ASUKF", Aerospace science and technology, vol. 22, **(2012)**, pp. 19-23.
[12] Y. Teng, J. Wang and Q. Huang, "Mathematical minimum of geometric dilution of precision (GDOP) for dual-GNSS constellations", Advances in space research, vol. 57, **(2016)**, pp. 183-188.
[13] Y. Wang, W. Zheng, S. Sun and L. Li, "X-ray pulsar based navigation using time-difference measurement", Aerospace science and technology, vol. 13, **(2014)**, pp. 27-35.

